



Facile synthesis of organically capped PbS nanoparticles

Ayorinde O. Nejo, Adeola A. Nejo, Rajasekhar V.S.R. Pullabhotla, Neerish Revaprasadu *

Department of Chemistry, University of Zululand, Private Bag X1001, Kwadlangezwa, South Africa

ARTICLE INFO

Article history:

Received 20 February 2012

Received in revised form 4 May 2012

Accepted 6 May 2012

Available online 12 May 2012

Keywords:

PbS nanoparticles

Lead sources

Hexadecylamine

Tri-n-octylphosphine oxide

Oriented attachment

ABSTRACT

PbS nanocubes and nanorods were successfully synthesized through a facile route using hexadecylamine (HDA) and tri-n-octylphosphine oxide (TOPO) as surfactants. The structure and morphology of the as-prepared PbS nanocrystals were characterized by X-ray diffraction (XRD), transmission electron microscopy (TEM), high resolution TEM. The morphology of the PbS was influenced by the variation in lead source and organic surfactant. Particles in the shape of spheres, perfect cubes and rods were obtained by variation in reaction conditions. A possible growth mechanism to explain the formation of these PbS nanocubes and nanorods is also discussed.

© 2012 Elsevier B.V. All rights reserved.

1. Introduction

The influence of the shape and size of inorganic nanocrystals in determining their varying physical and chemical properties has led to increased attention in the morphological control of semiconductor nanoparticles [1–4]. Nanostructured materials have been studied extensively because of their unique size tunable properties and potential applications in various areas such as lasers, solar cells, light-emitting diodes, sensors, and catalysis [1–7]. One-dimensional nanostructures such as nanorods, nanowires, nanobelts and nanotubes, in particular offer fundamental opportunities for understanding the effect of size and dimensionality on their collective optical, magnetic, and electronic properties [8,9].

Lead sulphide (PbS) as a unique semiconductor material has been relatively studied in the past decade. As an important IV–VI group semiconductor, PbS has attracted considerable attention owing to its especially small direct band gap (0.41 eV) and larger excitation Bohr radius (18 nm) [10,11] and has been widely used in many fields such as Pb^{2+} ion-selective sensors, photography, IR detectors and solar absorbers [12–15]. One-dimensional PbS nanoparticles have been applied in electroluminescent devices such as light emitting diodes [16,17] and optical devices such as optical switches due to the high third order nonlinear optical properties [18–20].

Many synthetic methods have been employed to prepare PbS nanoparticles. These include hydrothermal and solvothermal

methods [21,22], microwave-assisted heating [23], thermal decomposition methods [24], electrodeposition [25], template- and surfactant assisted methods [26,27] and hot injection precursor methods [17,28–31]. The hot injection routes involve the injection of the lead salt and sulphur source into co-ordinating solvents. Monodisperse spherical-shaped PbS nanocrystals were successfully synthesized by the hot injection method using $PbCl_2$ –Oleylamine and sulphur–Oleylamine heterogeneous system under a mild reaction conditions [28]. The viscosity of the growth environment was tuned by changing the $PbCl_2$ –Oleylamine ratio which coerced the nanocrystals to grow in a more diffusion-controlled manner. Warner et al. prepared PbS nanoparticles with diverse shapes by using a combination of surfactants [30]. A related method is the single-source precursor approach whereby a metal complex is thermolysed in a high boiling point solvent [32–34]. This method allows for the adjustment of size and size distribution by controlling the reaction conditions. Very monodispersed cube shaped PbS nanocrystals were synthesized by a solvothermal single-source precursor method at mild reaction conditions [22]. Cheon et al. reported the synthesis of large PbS nanocrystals with different shapes by thermolysis of a single molecular precursor [34].

We have successfully synthesized PbTe nanoparticles in the form of spheres using a hybrid solution based high temperature route [35]. In this work we report further on this methodology and its extension to PbS. The method involves reacting sulphur, with sodium borohydride ($NaBH_4$) to produce sulphide ions; followed by the reaction with a lead salt. The effects of temperature, surfactants and lead sources on the morphologies of the final PbS nanocrystals were investigated.

* Corresponding author. Tel.: +27 35 902 6152; fax: +27 35 902 6568.

E-mail address: nrevapra@pan.uzulu.ac.za (N. Revaprasadu).

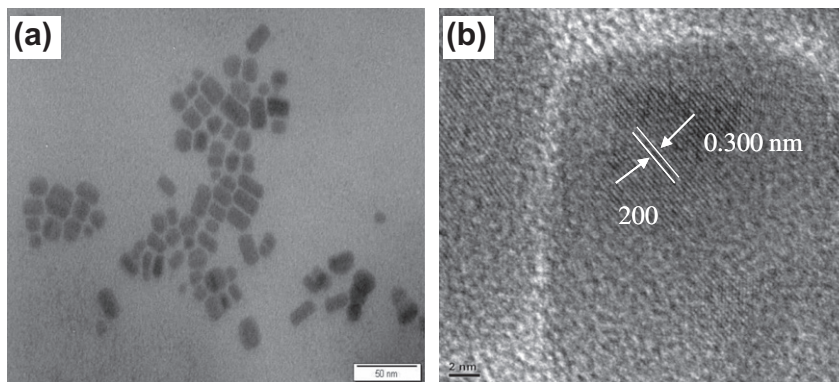


Fig. 1. (a) TEM image and (b) HRTEM image of PbS from PbCO_3 at 230 °C.

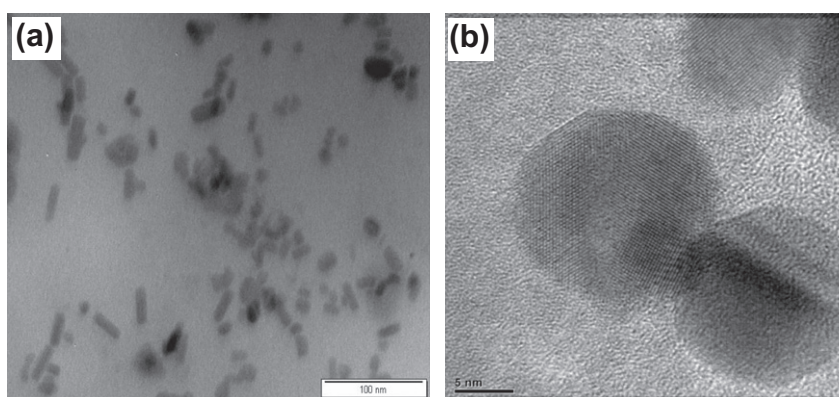


Fig. 2. (a) TEM image and (b) HRTEM image of PbS from $\text{Pb}(\text{NO}_3)_2$ at 230 °C.

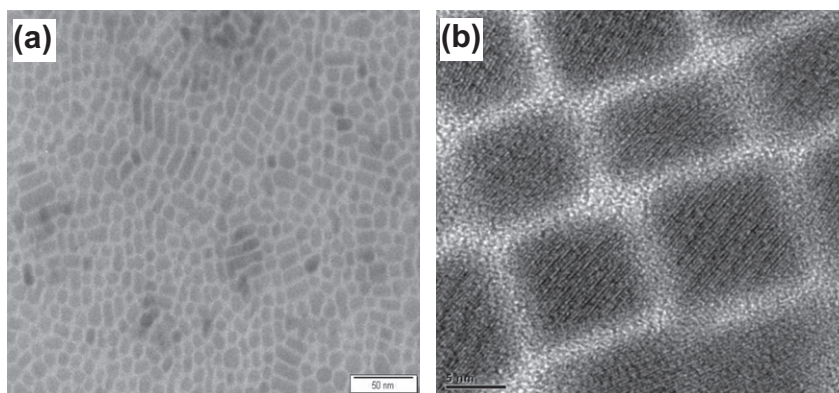


Fig. 3. (a) TEM image and (b) HRTEM image of PbS from PbSO_4 at 270 °C.

2. Materials and methods

2.1. Materials

All reagents and solvents were analytical grade and used without further purification. Hexadecylamine (HDA), tri-*n*-octylphosphine oxide (TOPO), and tri-*n*-octylphosphine (TOP) were purchased from Sigma–Aldrich. Methanol, lead nitrate, lead carbonate, lead sulphate and acetone were purchased from Saarchem, UnivAR, Merck chemicals.

2.2. Preparation of nanoparticles

In a typical procedure, 0.64 mmol of sulphur powder was mixed with 20.0 mL deionised water in a three necked flask. 1.58 mmol of NaBH_4 dissolved in 20.0 mL deionised water was added to this mixture and was left to stir for 12 h under nitrogen atmosphere at room temperature. 0.64 mmol of lead salt [PbSO_4 , $\text{Pb}(\text{NO}_3)_2$ and

PbCO_3] dissolved in 20.0 mL deionised water was added to the sulphide ion solution to give a brownish-black solution. The solution was stirred for 30 min followed by the addition of excess methanol. The resultant solution was then centrifuged and decanted to isolate the solid products which were dispersed into 6.0 mL of TOP and injected into hot HDA or TOPO (6 g) at temperatures of 190, 230 or 270 °C for 2 h. The reaction was quenched by adding excess methanol to the solution. The flocculate was separated from the supernatant by centrifugation. The resultant particles were dissolved in toluene for characterization.

2.3. Characterization

The phase of the material was identified by X-ray diffraction (XRD), employing a scanning rate of $0.05^\circ \text{min}^{-1}$ in a 2θ range from 20 to 80° , using a Bruker AXS D8 diffractometer equipped with nickel filtered $\text{Co K}\alpha$ radiation ($\lambda = 1.5418 \text{ \AA}$) at 40 kV, 40 mA at room temperature. The morphology and particle sizes of the samples were characterized by a JEOL 1010 TEM with an accelerating voltage of 100 kV,

Megaview III camera, and Soft Imaging Systems iTEM software. The detail morphological and structural features were investigated using JEOL 2010 HRTEM operated at an accelerating voltage of 200 kV.

3. Results and discussion

PbS was synthesized by the reduction of sulphur powder in water followed by the addition of different lead salts (nitrate, carbonate or sulphate) which act as the lead source. The PbS nanocrystals were grown by the thermolysis of the bulk material in hot HDA or TOPO which act as the solvent and surface passivating agent. The size and shape of the PbS nanocrystals was varied by changing the lead precursor sources, reaction temperatures and organic surfactants.

The PbS nanocrystals produced when the thermolysis was carried out in HDA were found to be well dispersed. Fig. 1a shows HDA capped PbS nanoparticles synthesized at 230 °C using PbCO_3 as the lead source. The PbS particles appear as unaggregated, monodispersed rods with an average width of 9 ± 2 nm and average length of 17 ± 5 nm. This result is consistent with previous work from our group on PbTe whereby nanorods of PbTe were obtained when PbCO_3 was used as lead source [34]. The HRTEM image of the PbS nanoparticles from the PbCO_3 source are shown in Fig. 1b. The HRTEM shows distinct lattice fringes with the lattice d-spacing of 0.30 nm, indexed to the (200) plane of cubic PbS.

When PbCO_3 was replaced by $\text{Pb}(\text{NO}_3)_2$ as the lead source and all other conditions kept constant, nanorods with irregular dimensions were obtained. There was some degree of aggregation or attachment of particles observed in the TEM image (Fig. 2a). The HRTEM

image (Fig. 2b) confirms the attachment of particles. There is a crystallographic alignment of two particles leading to the formation of an elongated particle. At 270 °C, the PbSO_4 source gave very uniform, monodispersed, self assembled cubic shaped particles with an average size of 7 ± 1 nm (Fig. 3a). The HRTEM image (Fig. 3b) confirms the regular cube shape. The self assembled PbS nanocubes had an average side-to-side of double-particle distance of about 1.8 nm as shown in Fig. 3b.

The use of three lead sources to produce particles with varying shapes can be explained by the probable different growth mechanisms. The PbS nanorods and nanocubes morphologies could be attributed to the HDA surfactant which provides a template for assembling the lead sulphide structures and making the crystals grow preferentially in a specific direction. The growth rates on the different facets in the system are dominated by the surface energy. For halite type crystals the {111} face with high surface energy grows faster than the lower-surface-energy {100} face which favours {100} facets leading to either nanocubes or nanorods. In the case of the PbCO_3 source, the insoluble nature of the carbonate results in a suspension of the undissolved cadmium carbonate which selectively adheres to the surface of the PbS nanoparticles thereby accentuating the difference in the growth rate between the crystallographic phases. This results in kinetically induced anisotropic growth. These results are similar to those of CdTe nanoparticles synthesized under the same reaction conditions [36].

When the lead source is $\text{Pb}(\text{NO}_3)_2$, there is evidence of growth by an oriented attachment process. Oriented aggregation (OA) is a special case in which the secondary particles are new single crystals composed of oriented primary particles [37,38]. This mecha-

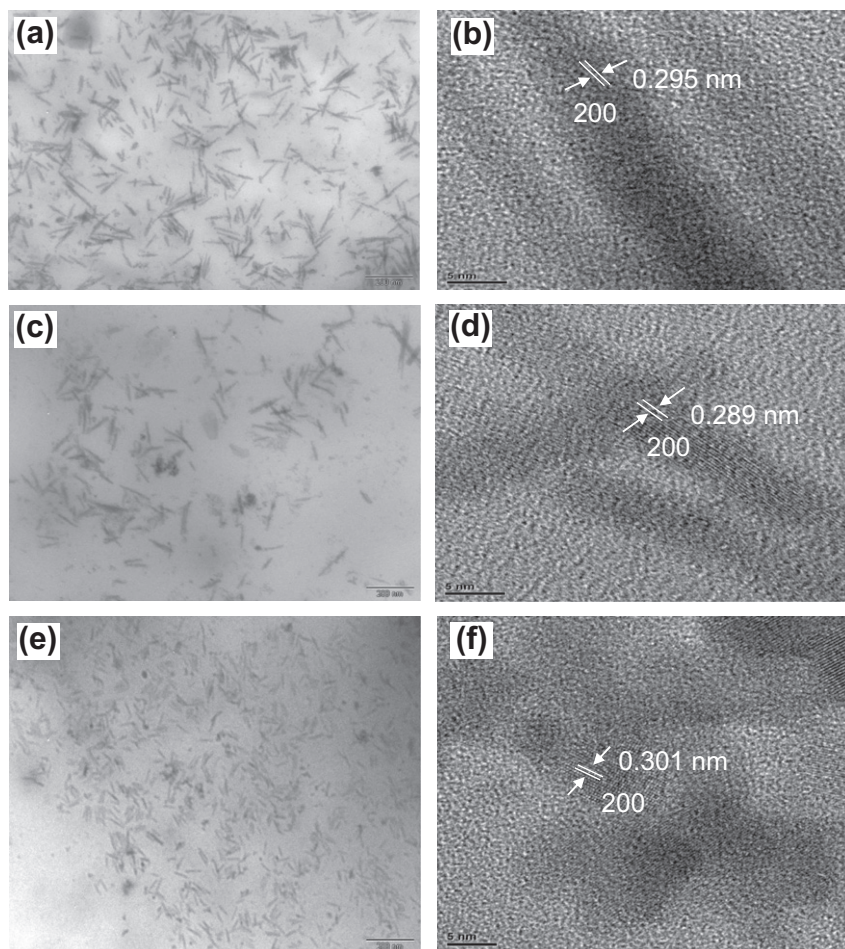


Fig. 4. TEM and HRTEM images (a and b) PbS nanocrystal from PbCO_3 at 230 °C; (c and d) PbS from $\text{Pb}(\text{NO}_3)_2$ at 230 °C and (e and f) PbS from PbSO_4 at 190 °C.

nism is based on the spontaneous self-organization of adjacent nanocrystals, resulting in growth by the coalescence of primary particles that share a common crystallographic orientation. Nanocrystal growth via the oriented attachment mechanism generally leads to the formation of anisotropic nanocrystals and particles of irregular shapes, as well as nanocrystals with defects. The HRTEM image (Fig. 2b) shows two particles attached to each other. The TEM image also shows the fusion of particles resulting in elongated particles. The PbSO_4 source gave perfect cube shaped particles which is the most thermodynamically stable morphology of PbS.

Recent studies have shown that selective anisotropic growth between different crystallographic surfaces can be adjusted by the use of appropriate absorbing organic surfactants [22]. It is well known that, the presence of the surfactant could kinetically control the relative growth rates of different crystal planes by allowing the growth along one facet to proceed while inhibiting the growth along another facet [34]. To explore the influence of the organic surfactant on the morphologies of PbS nanocrystals under otherwise similar reaction conditions, TOPO another organic capping agent was used in the place of HDA. TOPO is expected to exhibit different interaction with certain PbS crystal facets due to its phosphine functional group. The lead salts, PbCO_3 , $\text{Pb}(\text{NO}_3)_2$ and PbSO_4 were also used as lead sources. Thermolysis was carried out at a

temperature of 230 °C for PbCO_3 and $\text{Pb}(\text{NO}_3)_2$ sources while that of PbSO_4 source was carried out at 190 °C.

The TEM image (Fig. 4a) reveals that the PbS nanocrystals prepared from the PbCO_3 source are rod-shaped and the average diameter of these rods is about 12 ± 2 nm and average length of 90 ± 24 nm. It is obvious from the above measurements that the largest variation in the size of the PbS nanorods is due to the length variations. This may be due to the fact that the PbS nanorods grow along their length axis and that the different growth rate of the length within the ensemble resulted in slightly different lengths of the nanorods. Similar morphology were also observed in PbS nanocrystals prepared using $\text{Pb}(\text{NO}_3)_2$ and PbSO_4 as the lead sources.

The obtained PbS nanocrystals are rod-like in shape with average diameters of 7 ± 2 and 11 ± 2 nm and average lengths of 65 ± 22 and 62 ± 11 nm, respectively as shown in Fig. 4c and e. Fig. 4b, d and f show the HRTEM images of the PbS nanorods formed from the various lead precursors. The lattice spacing was found to be about 0.295, 0.289 and 0.301 nm for the PbS nanorods formed from PbCO_3 , $\text{Pb}(\text{NO}_3)_2$ and PbSO_4 , respectively. These d-spacing was indexed as (200) plane of cubic PbS. From the HRTEM images of all samples there appears to be no discontinuities in the lattice fringes indicating a perfect crystal. The formation of these anisotropic PbS nanoparticles suggest that the nucleation and

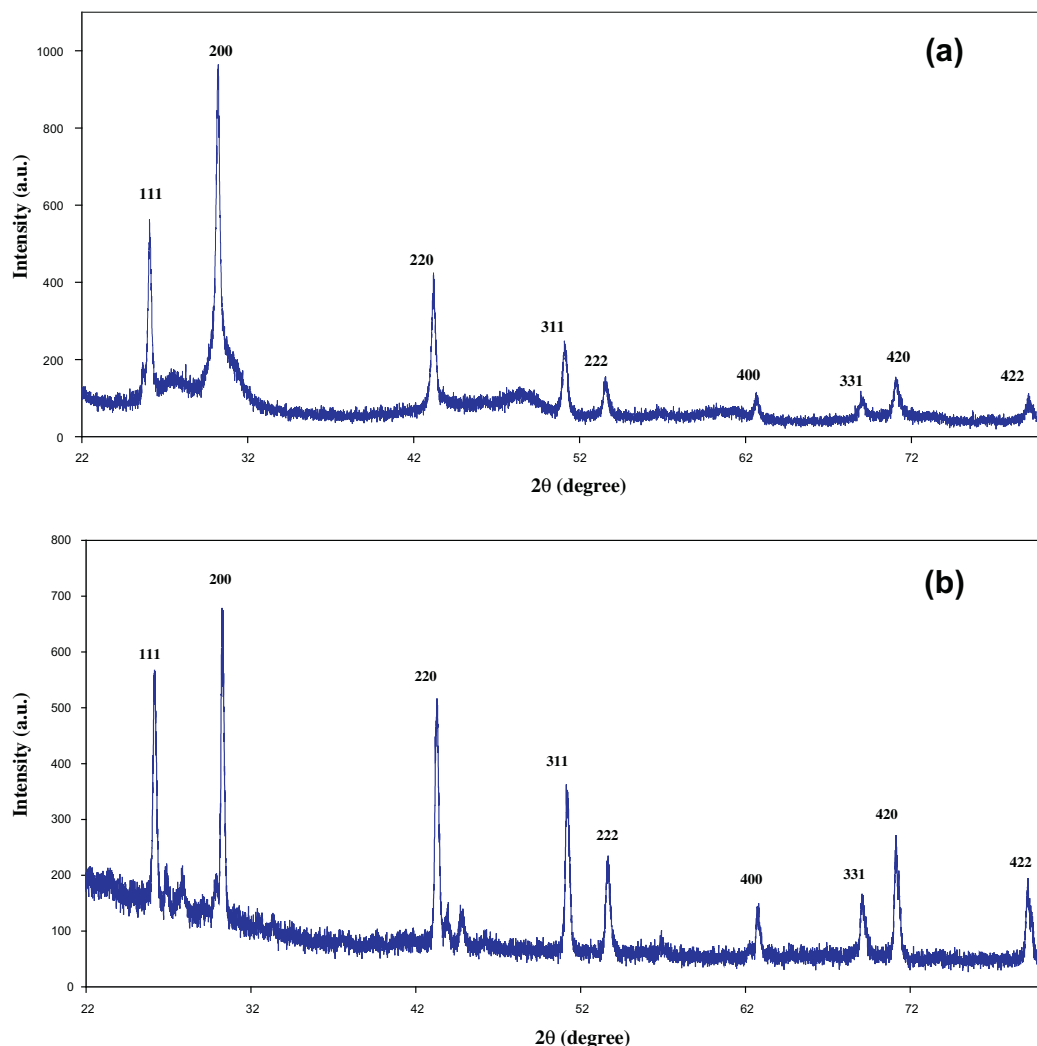


Fig. 5. XRD patterns of the PbS nanocrystals from $\text{Pb}(\text{NO}_3)_2$ at 230 °C: (a) HDA capped PbS nanocrystals and (b) TOPO capped PbS nanocrystals.

growth of PbS nanoparticles are well controlled by the nature of surfactant (TOPO). The anisotropic nature of the TOPO capped PbS nanoparticles could be due to the impurities present in the technical grade TOPO. It is well known that impurities such as hexylphosphonic acid (HPA) facilitate the growth of anisotropic CdSe nanoparticles [39]. The HPA binds selectively to a specific axis thereby inhibiting growth along other facets favouring rod-like single crystal growth, with preferred growth along the length axis.

The crystallinity of the as-prepared PbS nanocrystals were investigated by X-ray diffraction (XRD) are shown in Fig. 5. The results of the XRD patterns of the HDA and TOPO capped PbS nanocrystals prepared from $\text{Pb}(\text{NO}_3)_2$ indicate that samples were crystalline and the patterns are in good agreement with the bulk PbS crystal. The major diffraction peaks could be indexed as (111), (200), (220), (311), (222), (400), (331), (420), and (422) planes of cubic PbS, which is consistent with values reported in the literature [21,29,40].

4. Conclusion

HDA and TOPO capped PbS nanoparticles have been synthesized via a simple hybrid solution based thermolysis route. By varying the lead source HDA capped particles with morphologies ranging from close to spheres, elongated particles and perfect cubes were formed. When the capping group was changed to TOPO, predominantly rod shaped particles were obtained. The growth mechanism for the anisotropic HDA capped PbS is mostly likely due an oriented attachment mechanism. The formation of the rod shaped TOPO capped PbS is due to the impurities in TOPO. The X-ray diffraction and high resolution electron microscopy studies show that the particles are crystalline.

Acknowledgements

This work was supported by the Department of Science and Technology (DST) and National Research Foundation (NRF) of South Africa through the DST/NRF South African Research Chairs Initiative (SARCHI) program. The authors also acknowledge the Electron Microscopy Unit, University of Kwa-Zulu Natal for the TEM and the CSIR, Pretoria for the HRTEM facilities.

References

- [1] C.B. Murray, C.R. Kagan, M.G. Bawendi, *Annu. Rev. Mater. Sci.* 30 (2000) 545–610.
- [2] A. Bachtold, P. Hadley, T. Nakanishi, C. Dekker, *Science* 294 (2001) 1317–1320.
- [3] Y.Q. Gao, Y. Bando, *Nature* 415 (2002) 599.
- [4] J.Z. Zhang, *J. Phys. Chem. B* 104 (2000) 7239–7253.
- [5] V.I. Klimov, A.A. Mikhailovsky, D.W. McBranch, C.A. Leatherdale, M.G. Bawendi, *Science* 287 (2000) 1011–1013.
- [6] J.T. Hu, L.S. Li, W.D. Yang, L. Manna, L.W. Wang, A.P. Alivisatos, *Science* 292 (2001) 2060–2063.
- [7] N. Tessler, V. Medvedev, M. Kazes, S.H. Kan, U. Banin, *Science* 295 (2002) 1506–1508.
- [8] Z.W. Pan, Z.R. Dai, Z.I. Wang, *Science* 291 (2001) 1947–1949.
- [9] J. Hu, T.W. Odom, C.M. Lieber, *Acc. Chem. Res.* 32 (1999) 435–445.
- [10] D.E. Aspnes, M. Cardona, *Phys. Rev.* 173 (1968) 714–728.
- [11] J.L. Machol, F.W. Wise, R.C. Patel, D.B. Tanner, *Phys. Rev. B* 48 (1993) 2819–2822.
- [12] P.K. Nair, O. Gomezdaza, M.T.S. Nair, *Adv. Mater. Opt. Electron.* 1 (1992) 139–145.
- [13] T.K. Chaudhuri, S. Chatterjee, *Proc. Int. Conf. Thermoelectr.* 11 (1992) 40.
- [14] P. Gadenne, G. Deutscher, *J. Appl. Phys.* 66 (1989) 3019–3025.
- [15] H. Hirata, K. Higashiyama, *Bull. Chem. Soc. Jpn.* 44 (1971) 2420–2423.
- [16] L. Levina, V. Sukhovatkin, S. Musikhin, S. Cauchi, R. Nisman, D.P. Bazett-Jones, E.H. Sargent, *Adv. Mater.* 17 (2005) 1854–1857.
- [17] M.A. Hines, G.D. Scholes, *Adv. Mater.* 15 (2003) 1844–1849.
- [18] Y. Wang, *Acc. Chem. Res.* 24 (1991) 133–135.
- [19] S. Jing, S. Xing, Y. Wang, H. Hu, B. Zhao, C. Zhao, *Mater. Lett.* 62 (2008) 977–979.
- [20] C. Li, G. Shi, H.Y. Xu, S.Y. Guang, R.H. Yin, Y.L. Song, *Mater. Lett.* 61 (2007) 1809–1811.
- [21] D. Liang, S. Tang, J. Liu, J. Liu, X. Lv, L. Kang, *Mater. Lett.* 62 (2008) 2426–2429.
- [22] T. Duan, W. Loua, X. Wang, Q. Xuea, *Colloid Surf. A: Physicochem. Eng. Aspects* 310 (2007) 86–93.
- [23] J. Sun, X. Shen, L. Guo, K. Chen, Q. Liu, *Physica E* 41 (2009) 1527–1532.
- [24] Z. Zhao, K. Zhang, J. Zhang, K. Yang, C. He, F. Dong, B. Yang, *Colloid Surf. A: Physicochem. Eng. Aspects* 355 (2010) 114–120.
- [25] D. Kumar, G. Agarwal, B. Tripathi, D. Vyas, V. Kulshretha, *J. Alloys Compd.* 484 (2009) 463–466.
- [26] Y. Liu, D. Hou, G. Wang, *Chem. Phys. Lett.* 379 (2003) 67–73.
- [27] Y. Yu, F.P. Du, J.C. Yu, Y.Y. Zhuang, P.K. Wong, *J. Solid State Chem.* 177 (2004) 4640–4647.
- [28] L. Cademartiri, J. Bertolotti, R. Sapienza, D.S. Wiersma, G. Freymann, G.A. Ozin, *J. Phys. Chem. B* 110 (2006) 671–673.
- [29] J. Liu, H. Yu, Z. Wu, W. Wang, J. Peng, Y. Cao, *Nanotechnology* 19 (2008) 345602.
- [30] J.H. Warner, E. Thomson, A.R. Watt, N.R. Heckenberg, H. Rubinsztein-Dunlop, *Nanotechnology* 16 (2005) 175–179.
- [31] J. Joo, H.B. Na, T.Y. Yu, J.H. Yu, Y.W. Kim, F. Wu, J.Z. Zhang, T. Hyeon, *J. Am. Chem. Soc.* 125 (2003) 11100–11105.
- [32] T. Trindade, P. O'Brien, X. Zhang, M. Motevalli, *J. Mater. Chem.* 7 (6) (1997) 1011–1016.
- [33] J. Akhtar, M.A. Malik, P. O'Brien, M. Helliwell, *J. Mater. Chem.* 20 (2010) 6116–6124.
- [34] S.M. Lee, Y.W. Yun, S.N. Cho, J. Cheon, *J. Am. Chem. Soc.* 124 (2002) 11244–11245.
- [35] N. Ziqubu, K. Ramasamy, P.V.S.R. Rajasekhar, N. Revaprasadu, P. O'Brien, *Chem. Mater.* 12 (2010) 3817–3819.
- [36] N. Mntungwa, P.V.S.R. Rajasekhar, N. Revaprasadu, *Mater. Chem. Phys.* 126 (2011) 500–506.
- [37] Y.-W. Jun, J.-H. Lee, J.-S. Choi, J. Cheon, *J. Phys. Chem. B* 109 (2005) 14795–14806.
- [38] A.P. Alivisatos, *Science* 289 (2000) 736–737.
- [39] L. Manna, E.C. Scher, A.P. Alivisatos, *J. Am. Chem. Soc.* 122 (2000) 12700–12706.
- [40] S.M. Lee, S.N. Cho, J. Cheon, *Adv. Mater.* 15 (2003) 441–444.